S-wave resonance coupled-channel approach to the reactions $\pi^- + p \rightarrow \eta + n$ and $K^- + p \rightarrow \eta + \Lambda$, and a determination of the ηn and $\eta\Lambda$ scattering lengths

V. V. Abaev
St. Petersburg Institute of Nuclear Physics, Gatchina, Russia

B. M. K. Nefkens
University of California, Los Angeles, California 90095
(Received 21 November 1994)

The total cross sections of the reactions $\pi^- + p \rightarrow \eta + n$ and $K^- + p \rightarrow \eta + \Lambda$ near threshold have been calculated in an *S*-wave resonance coupled-channel approach. The ηN scattering length is $[0.621 \pm 0.040 + i(0.306 \pm 0.034)]$ fm and the $\eta\Lambda$ scattering length is $[0.64 \pm 0.29 + i(0.80 \pm 0.30)]$ fm. The large value of the $\eta\Lambda$ scattering length leads us to speculate on the possible existence of η-mesic hypernuclei.

PACS number(s): 13.75.Gx, 13.75.Jz, 21.80.+a, 25.80.−e

I. INTRODUCTION

η production is of special interest for several reasons.

(a) The isospin of the η is $I=0$. So, η production is isospin-selective which facilitates the studies of baryon spectroscopy [1]. For example, in the reaction $\pi^- + p \rightarrow \eta + n$ only $N(I=1/2)$ resonances are excited. In contrast, πN elastic scattering involves a mixture of $N(I=1/2)$ and $\Delta(I=3/2)$ states. Of particular interest is the threshold region where one expects mainly *S*-wave production. It is remarkable that η threshold production by pions and photons is dominated by an *S*-wave resonance, the $S_{11}(1535)$, which has an unexpectedly large η branching ratio [2]. η production by K^- shows similar features: there is a strong S_{01} resonance, the $\Lambda(1670)$, very close to threshold; there is also an S_{21} resonance, the $\Sigma(1750)$, which is very close to the $\eta\Sigma$ threshold [2]. We may expect that the simplest *S*-wave resonance approach is acceptable and that we can get several *S*-wave resonance parameters just from η production data.

(b) The ηN scattering length is of particular interest to nuclear physics because the *S*-wave ηN interaction is large and attractive. It has been proposed that a large scattering length, $a_{\eta N} \geqslant 0.3$ fm, could lead to a new type of nuclear matter, hadronically bound η-mesic nuclei [3]. In the same spirit we like to discuss the possibility of even more exotic systems, the η-mesic hypernuclei. The scattering length is obtained from η production data near threshold which is straightforward in a coupled-channel approach.

II. THE *S*-WAVE RESONANCE COUPLED-CHANNEL MODEL

Consider meson-nucleon (mN) interactions, such as πN or KN scattering, for the special case of an *S*-wave resonance. Furthermore, a sharp, inelastic two-body channel such as η production,

$$\pi^- + p \rightarrow \eta + n, \tag{1}$$

$$K^- + p \rightarrow \eta + \Lambda, \tag{2}$$

opens not too far from the resonance pole. The opening of such a channel causes a cusp in the elastic channel. In the speed plot of the elastic *S*-wave amplitude this shows up as an extra nonresonant peak which is likely to disturb the *S*-wave resonance shape. The above case is described by three amplitudes

$$A(mN \rightarrow mN), \tag{3}$$

$$A(mN \rightarrow \eta N) \quad \text{or} \quad A(mN \rightarrow \eta\Lambda), \tag{4}$$

$$A(\eta N \rightarrow \eta N) \quad \text{or} \quad A(\eta\Lambda \rightarrow \eta\Lambda). \tag{5}$$

The resonance part of these amplitudes may be written in simple Breit-Wigner form

$$T_1(W) = \frac{\Gamma_1/2}{(W_0 - W) - i\Gamma_t/2} = \frac{\eta_r(W) e^{2i\delta_{r_1}(W)} - 1}{2i}, \tag{6}$$

$$T_2(W) = \frac{\sqrt{\Gamma_1 \Gamma_2}/2}{(W_0 - W) - i\Gamma_t/2} = \frac{\sqrt{1 - \eta_r^2(W)}\, e^{i[\delta_{r_1}(W) + \delta_{r_2}(W)]}}{2i}, \tag{7}$$

$$T_3(W) = \frac{\Gamma_2/2}{(W_0 - W) - i\Gamma_t/2} = \frac{\eta_r(W) e^{2i\delta_{r_2}(W)} - 1}{2i}, \tag{8}$$

where W is the invariant energy, W_0 the mass of the resonance, Γ_t the total width of the resonance, Γ_1 and Γ_2 are the partial widths of the first and second channels and $\Gamma_t = \Gamma_1 + \Gamma_2$.

For elastic scattering, the amplitude (6) is not a real partial wave amplitude obtained from phase shift analysis, e.g., the S_{11} wave in πN scattering. It is only the resonance part of it. For example, if

$$T(W) = \frac{\eta_r(W)\, \eta_b(W) e^{2i[\delta_r(W) + \delta_b(W)]} - 1}{2i}, \tag{9}$$

where $\delta_r(W)$ and $\delta_b(W)$ are the resonance and background phases, $\eta_r(W)$ and $\eta_b(W)$ are the resonance and background inelasticity parameters, the resonance part is given by (6). This means that with Eq. (6) we describe only the resonance

0556-2813/96/53(1)/385(5)/$06.00

part of the elastic scattering amplitude. The amplitudes (7) and (8) should be the proper ones according to our approach, in which there is only one resonance and no background.

One can see from Eq. (7) that the cross sections of the reactions (1) and (2) do not depend on the phases and are proportional only to $(1-\eta_r^2)$. This means that the coupling between elastic scattering and production reactions is given only by the inelasticity (absorption) parameter η_r, and it is not necessary to describe the phase shifts (or real and imaginary parts) of the elastic amplitude (6) or (9). One needs to know only the inelasticity parameter.

The partial widths have a specific energy dependence. In the relativistic approach for an S wave [4] they are

$$\Gamma_i(W)=\Gamma_i(W_0)\,\frac{2W_0}{W_0+W}\,\frac{q_i}{q_{i0}}, \tag{10}$$

where q_i is the c.m. momentum of the ith channel and q_{i0} is the c.m. momentum at resonance $(W=W_0)$.

The resonance decay branching fractions are just the ratios of the partial widths to the total width at resonance (for the elastic channel it is the elasticity) $X_i=\Gamma_i(W_0)/\Gamma_t(W_0)$, with $X_1+X_2=1$.

Now let us consider a third important channel, $mN\rightarrow\pi mN$. Then the only modification of Eqs. (6)–(8) will be in the denominators. We have to add the third part to the total width,

$$\Gamma_t(W)=\Gamma_1(W)+\Gamma_2(W)+\Gamma_3(W) \tag{11}$$

and

$$X_1+X_2+X_3=1. \tag{12}$$

The energy dependence of the three-particle final state can be incorporated in the manner discussed by Cutkosky [5] or Manley [6].

The above scenario describes the case of pion and kaon interactions around $p_{\mathrm{lab}}\approx 750$ MeV/c where we have only three important channels: $\pi N\rightarrow\pi N, \pi N\rightarrow\eta N, \pi N\rightarrow 2\pi N$ and $KN\rightarrow KN, KN\rightarrow\eta\Lambda, KN\rightarrow\pi\Sigma$. Other reactions are small and can be ignored. In both cases we have four free parameters: W_0, $\Gamma_t(W_0)$, X_1, and X_2, since X_3 is imposed by (12).

For the πN interaction we can impose an additional constraint coming from the inelastic $2\pi N$ scattering channels. The two-pion decay mode of the S_{11} resonance has $X_3\leqslant 0.10$ [2]. This value is based on the results of the elastic phase shift analyses of Refs. [5,7] and double-pion production analysis [6]. The resonance part of this amplitude has the same form as (7),

$$T_4(W)=\frac{\sqrt{\Gamma_1\Gamma_3}/2}{(W_0-W)-i\Gamma_t/2}, \tag{13}$$

and can be used for the analysis of two-pion production data [6]. The Breit-Wigner formula for the inelasticity parameter may be obtained from Eq. (6)

$$\eta_r(W)=\sqrt{1-\frac{\Gamma_{\pi N}(W)[\Gamma_{\eta N}(W)+\Gamma_{2\pi N}(W)]}{(W_0-W)^2+[\Gamma_t^2(W)/4]}}. \tag{14}$$

This formula has a very simple interpretation: the product $\Gamma_{\pi N}(W)\Gamma_{\eta N}(W)$ represents the ηN decay channel and the product $\Gamma_{\pi N}(W)\Gamma_{2\pi N}(W)$ represents the $2\pi N$ decay channel. Below the η production threshold $\Gamma_{\eta N}(W)=0$ and in Eq. (14) the product $\Gamma_{\pi N}(W)\Gamma_{2\pi N}(W)\approx 0$ and $\eta_r(W)\approx 1$. For the $2\pi N$ decay channel the partial inelasticity parameter [6] is given by the same Eq. (14) with $\Gamma_{\eta N}(W)=0$ in the numerator.

The total cross section in mb for reactions (1) and (2) is

$$\sigma_t(W)=\frac{4\pi}{q_1^2}\,C\times 0.3894\times 10^6|T_2(W)|^2, \tag{15}$$

where the isospin coefficient $C=2/3$ and 1/2, respectively, and

$$|T_2(W)|^2=\frac{1}{4}\,\frac{\Gamma_{\pi N}(W)\Gamma_{\eta N}(W)}{(W_0-W)^2+[\Gamma_t^2(W)/4]}$$
$$=\frac{[1-\eta_r^2(W)]}{4}\,\frac{\Gamma_{\eta N}(W)}{\Gamma_{\eta N}(W)+\Gamma_{2\pi N}(W)}. \tag{16}$$

The scattering length of the ηN or $\eta\Lambda$ elastic amplitude (8) is given by

$$\lim_{q_2\rightarrow 0}[T_3(W)/q_2]=\mathrm{Re}a_0+i\ \mathrm{Im}a_0. \tag{17}$$

In the limit $q_2\rightarrow 0$, one can represent the scattering length in terms of resonance parameters. If we use the approximation suggested by Liu [8]

$$\Gamma_t(q_2\rightarrow 0)=\Gamma_1(W_0)+\Gamma_3(W_0), \tag{18}$$

then the scattering length is given by

$$a_0=\frac{X_2}{q_2}\left[\frac{W_0^2-W_{\mathrm{th}}^2}{W_0\Gamma_t(W_0)}-i(1-X_2)\right]^{-1}, \tag{19}$$

where W_{th} is the invariant energy at threshold.

III. RESULTS

Shown in Fig. 1 are the results of our coupled-channel parametrization of the reactions under consideration. The total cross sections $\sigma_t(\pi^-+p\rightarrow\eta+n)$ and $\sigma_t(K^-+p\rightarrow\eta+\Lambda)$ are taken from Refs. [9,10]. For $\pi^-+p\rightarrow\eta+n$ we use the star-evaluated data base of Ref. [9]. The data points close to threshold are obtained using the partial cross section value of Binnie *et al.* [11] assuming S-wave dominance. The inelasticity parameters of πN scattering are taken from the phase-shift analyses of CMU [5], PNPI [12], and Saclay [13]. The partial inelasticity parameters of the $2\pi N$ channel are taken from the phase-shift analysis of Ref. [14]. For KN scattering we applied the constraint from the PDT [2] for $X_{KN}=0.20\pm0.05$ (Table I).

Bhandari and Chao [15] have made an analysis of the $S_{11}(1535)$ parameters using the accurate π^-p backward elastic scattering data which has a cusplike structure near the ηN threshold. Their results, $W_0=1547\pm6$ MeV, $\Gamma_t(W_0)=139\pm33$ MeV, and $X_{\pi N}=0.297\pm0.026$ are in good agreement with our values shown in Table I. The value $X_{\eta N}=0.59$

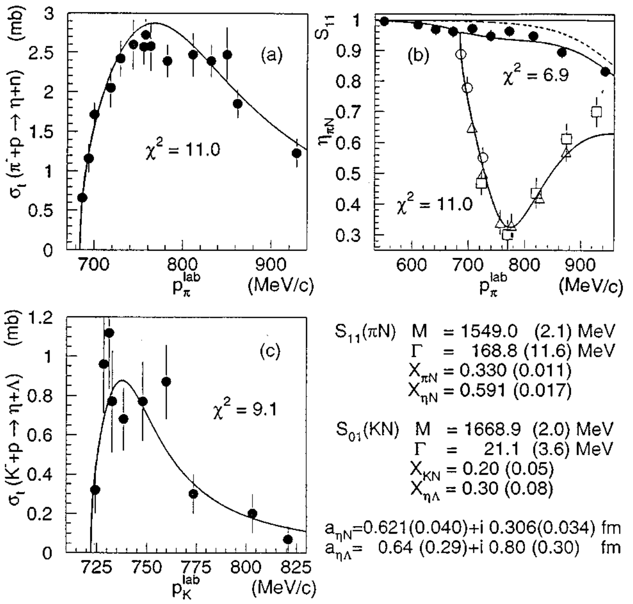

FIG. 1. (a) Experimental results for $\sigma_t(\pi^- + p \to \eta + n)$ from Ref. [9] and the result of our parametrization. (b) Results of the phase shift analyses from Ref. [5] (open squares), Ref. [12] (open circles), Ref. [13] (triangles), Ref. [14] (black dots), and the results of our fit. The dashed curve represents the partial inelasticity parameter from $S_{11}(1650)$. (c) Experimental results for $\sigma_t(K^- + p \to \eta + \Lambda)$ from Ref. [10] and the result of our parametrization.

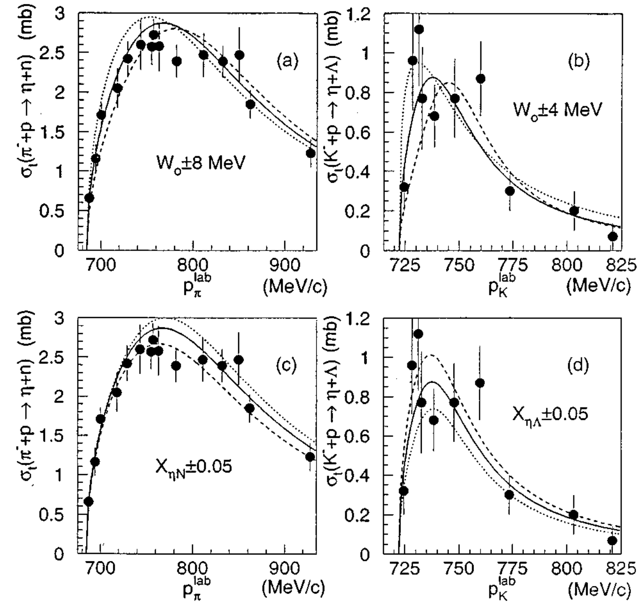

FIG. 2. (a) Experimental results for $\sigma_t(\pi^- + p \to \eta + n)$ from Ref. [9] compared to a Breit-Wigner shape for W_0=1541 MeV (dotted), W_0=1549 MeV (solid), and W_0=1557 MeV (dashed line) with $\Gamma_t(W_0)$=169 MeV and $X_{\eta N}$=0.59. (b) Same as (a) for $\sigma_t(K^- + p \to \eta + \Lambda)$ from Ref. [10]; W_0=1665 MeV (dotted), W_0=1669 MeV (solid), and W_0=1673 MeV (dashed) with $\Gamma_t(W_0)$=21 MeV and $X_{\eta\Lambda}$=0.30. (c) Variation of the $S_{11}(1549)$ Breit-Wigner curve with the elasticity; $X_{\eta N}$=0.64 (dashed), $X_{\eta N}$=0.59 (solid), and $X_{\eta N}$=0.54 (dotted) with W_0=1549 MeV and $\Gamma_t(W_0)$=169 MeV. (d) Same as (c) for $S_{01}(1669)$; $X_{\eta\Lambda}$=0.35 (dashed), $X_{\eta\Lambda}$=0.30 (solid), and $X_{\eta\Lambda}$=0.25 (dotted) with W_0=1669 MeV and $\Gamma_t(W_0)$=21 MeV.

is consistent with the experimental data contrary to Liu's conclusion [8].

The sensitivity to the resonance mass and to the elasticity is shown in Fig. 2. Figure 3 shows the Argand plots of the elastic ηN and $\eta\Lambda$ amplitudes. One can see a reliable-looking resonance circle for each amplitude.

The dependence of the real and imaginary parts of the dimensional amplitudes of Eq. (17) on the c.m. variable q_2^2 is given in Fig. 4 for three values of the mass of the resonance. This figure shows that a better determination of the resonant mass can substantially improve the accuracy of the scattering lengths. Note that the nearer the pole of the resonance is to the threshold, the larger the sensitivity of the scattering length is to the resonance parameters and the more nonlinear is the behavior of the amplitudes near threshold. Considering that the $\Lambda(1670)$ resonance is much closer to threshold than the $S_{11}(1535)$ in the c.m. momentum scale (ReT=0) and very narrow, the S-wave dominance assumption is reliable

TABLE I. Resonance parameters used in calculating the curves of Figs. 1–4. Also shown are the parameters X_i of the PDT [2].

Symbol	Notation	Mass	Width	X_i	Mode	X_i
$N(1535)$	S_{11}	1549	169	0.33	πN	0.35–0.55
				0.59	ηN	0.45–0.55
				0.08	$2\pi N$	$\leqslant$0.1
$\Lambda(1670)$	S_{01}	1669	21	0.20	KN	0.15–0.25
				0.30	$\eta\Lambda$	0.15–0.35
				0.50	$\pi\Sigma$	0.20–0.60

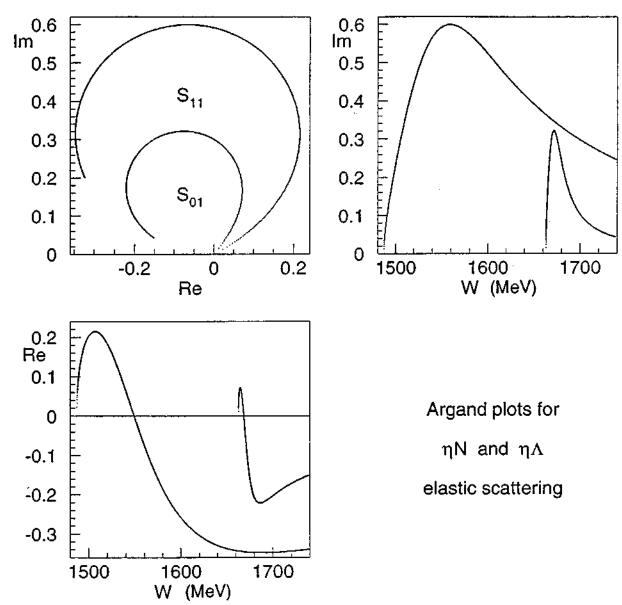

FIG. 3. Argand plots for the ηN elastic scattering S_{11} amplitude and the $\eta\Lambda$ elastic scattering S_{01} amplitude for the parameters of Table I.

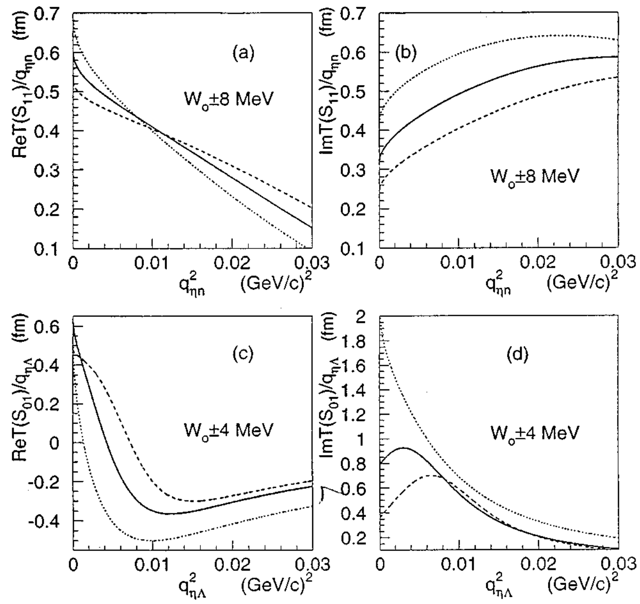

FIG. 4. Re$T(S_{11})/q_{\eta n}$ (a) and Im $T(S_{11})/q_{\eta n}$ (b) as a function of $q^2_{\eta n}$ and Re$T(S_{01})/q_{\eta\Lambda}$ (c) and Im $T(S_{01})/q_{\eta\Lambda}$ (d) as a function of $q^2_{\eta\Lambda}$ for the Breit-Wigner resonances from Fig. 2.

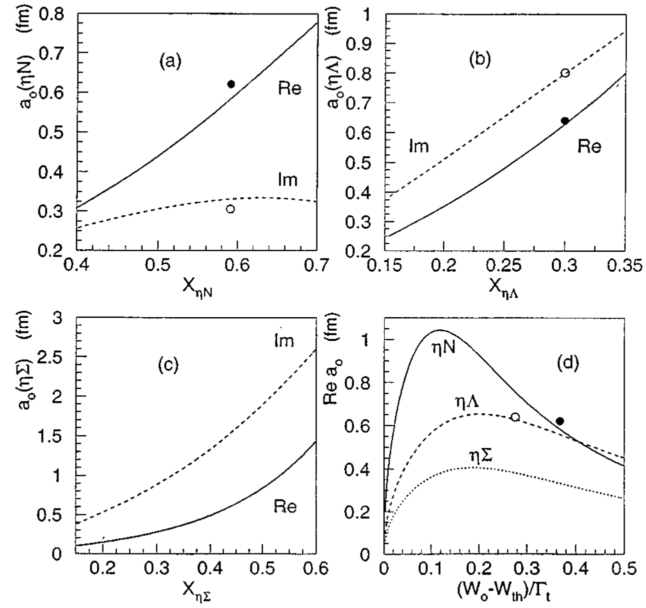

FIG. 5. Real and imaginary parts of the ηN (a), $\eta\Lambda$ (b), and $\eta\Sigma$ (c) scattering lengths as a function of the elasticity given by Eq. (19); the parameters are given in Table I. For $\eta\Sigma$ scattering the mass is $W_0=1750$ MeV and the width is $\Gamma_t(W_0)=90$ MeV. (d) Mass dependence of the real parts of the scattering lengths. For $\eta\Sigma$ scattering, $X_{\eta\Sigma}=0.35$. The points are the exact calculations.

above the resonance and we expect that the resonance parameters can be extracted rather reliably from the production cross section.

For πN scattering we have taken into account the tail of the second $S_{11}(1650)$ resonance with the $2\pi N$ branching fractions from Ref. [6]. In this case we have multiplied the inelasticity parameter of the $S_{11}(1535)$ resonance (14) by the same expression for the $S_{11}(1650)$. This was done according to the formalism of Ref. [6]. The corresponding part of the partial inelasticity parameter is shown in Fig. 1 by the dashed line. The $2\pi N$ branching fractions for the $S_{11}(1535)$ resonance are also taken from Ref. [6].

Our results could be refined by considering the nonresonant background in the η production channel. We estimate the changes to be small and the accuracy of the existing data does not warrant a more elaborate analysis. Better data on η production is needed to resolve the inconsistencies of the existing data set. An experiment is under way at the AGS to obtain better σ_t and $d\sigma/d\Omega$ information [16]. For the KN interaction the experimental situation is much worse than for the πN interaction.

Our value of the ηN scattering length (Fig. 1) is consistent with the result of Wilkin [17], $a_{\eta N}=(0.476+i0.279)$ fm. The smaller value reported by Liu [3], $a_{\eta N}=(0.27+i0.22)$ fm, is related directly to his using a small $X_{\eta N}$ value. The large value given by Arima *et al.* [18], $a_{\eta N}=(0.98+i0.37)$ fm, is related to using a large η production cross section.

Our result for the $\eta\Lambda$ scattering length (Fig. 1) is a first determination and indicates that $\eta\Lambda$ and ηN scattering at threshold are not very different.

The calculations based on the convenient approximation of Eq. (19) give nearly the same results. In Figs. 5(a) and 5(b) one can see the dependence of the ηN and $\eta\Lambda$ scattering lengths on the value of the branching ratios, $X_{\eta N}$ and $X_{\eta\Lambda}$, for the masses and widths given in Table I. The points indicate the calculation based on Eq. (17).

The threshold of the reaction $K^- + p \rightarrow \eta + \Sigma^0$ is very close to the well-known $\Sigma(1750)$ resonance [$W_0=1750$ MeV, $\Gamma_t(W_0)=90$ MeV, $X_{\eta\Sigma}=0.15-0.55$]. According to the approximate calculations of Eq. (19) we find that the $\eta\Sigma$ scattering length in the S_{21} resonance approach has the lower and upper limits shown in Fig. 5(c),

$$a_{\eta\Sigma}=[0.10\text{–}1.10+i(0.35\text{–}2.20)] \text{ fm}. \tag{20}$$

If $X_{\eta\Sigma}\approx 0.5$ then one finds the same large attraction in the $\eta\Sigma$ interaction as in $\eta\Lambda$. The resonance mass dependence on the real part of the scattering lengths is shown in Fig. 5(d). The width and elasticity for the case of ηN and $\eta\Lambda$ scattering are taken from Table I. For $\eta\Sigma$ scattering they are $\Gamma_t(W_0)=90$ MeV and $X_{\eta\Sigma}=0.35$. One can see that the maximum value occurs when the resonance mass is very close to the threshold, $W_0 \approx W_{\rm th}+(0.1\text{–}0.25)\Gamma_t(W_0)$.

The large value of $a_{\eta N}$ enhances the likelihood for the existence of η-mesic nuclei proposed by Liu and others [3]. A search for this via the two-body reaction $\pi^+ + {}^{16}\mathrm{O} \rightarrow \mathrm{p} + {}^{15}_{\eta}\mathrm{O}$ has been unsuccessful [19]. This could be because the η-mesic nuclei have a large width. Another possibility is that the choice of the incident momentum of 800 MeV/c was too large; see Fig. 1(a). Above the resonance, the real part of the ηN amplitude turns from positive to negative, i.e., the ηN interaction becomes repulsive; see Fig. 3. The best momentum is near the threshold of the above reaction, where the η-nucleus c.m. momentum is small and the interaction is attractive. The important advantage of the threshold measurements is a zero degree detection of all outgoing particles, i.e., we measure the total cross section. We suggest to repeat the experiment at a lower incident momentum in the subthreshold region of reaction (1).

The finding that $a_{\eta\Lambda}$ is also large has prompted us to speculate on the possible existence of an even more exotic nuclear species, namely η-mesic hypernuclei. They can be searched for in a similar manner with a K^- beam

$$K^- + {}^{Z}A \to p + {}^{Z-2}_{\eta\Lambda}(A-1), \tag{21}$$

$$\to n + {}^{Z-1}_{\eta\Lambda}(A-1), \tag{22}$$

$$\to \pi^+ + {}^{Z-2}_{\eta\Lambda}A, \tag{23}$$

$$\to \pi^0 + {}^{Z-1}_{\eta\Lambda}A, \tag{24}$$

$$\to \pi^- + {}^{Z}_{\eta\Lambda}A. \tag{25}$$

In this case the mechanism is more difficult than in the pion-nucleus reaction and should have two stages: the production of an $\eta\Lambda$ pair on a nuclear proton (2) and the rescattering of the η and/or Λ on the second nucleon or virtual pion of the nucleus (spectator). The measurements should be performed in the threshold region of these reactions and in the subthreshold region of the reaction (2). We suggest the reaction

$$K^- + {}^{12}\mathrm{C} \to n + {}^{11}_{\eta\Lambda}\mathrm{B}, \tag{26}$$

because the ${}^{11}_{\Lambda}\mathrm{B}$ is a well-known hypernucleus with a large binding energy of 10.24 MeV.

There is an intriguing indication for the existence of a quasibound η-mesic nuclear state in the total cross section near threshold and in the 180° excitation function of $p+d \to \eta + {}^{3}\mathrm{He}$ [20]. Furthermore there is some evidence that the cross section of the reaction $\pi^- + {}^{3}\mathrm{He} \to \eta + {}^{3}\mathrm{H}$ [21] is also large and isotropic. The quasibound η-hypernuclear state could be found close to threshold of the reaction $K^- + {}^{Z}A \to \eta + {}^{Z-1}_{\Lambda}A$. We suggest to measure the excitation function of the reaction

$$K^- + {}^{4}\mathrm{He} \to \eta + {}^{4}_{\Lambda}\mathrm{H} \tag{27}$$

near threshold.

Finally we would like to mention that the η-mesic nuclei and hypernuclei could be observed by an indirect method like measuring the cusps in elastic pion and kaon-nucleus scattering. At the threshold of the above reactions one expects to see a threshold cusp and below it the anomaly caused by the η-mesic nucleus or hypernucleus. The shape and the magnitude are unpredictable and at some angles the cusp could disappear. This experiment is very simple, but it is not direct evidence for the η-mesic states.

[1] M. G. Huber and B. C. Metsch, in Proceedings Physics with Light Mesons and the Second International Workshop on πN Physics, Los Alamos, 1987, edited by W. R. Gibbs and B. M. K. Nefkens (Report No. LA-11184-C), p. 91.
[2] Particle Data Group, Phys. Rev. D **50**, 1173 (1994).
[3] R. S. Bhalerao and L. C. Liu, Phys. Rev. Lett. **54**, 865 (1985).
[4] H. Pilkuhn, *The Interaction of Hadrons* (North-Holland, Amsterdam, 1967); *Relativistic Particle Physics* (Mir, Moscow, 1983).
[5] R. E. Cutkosky, C. P. Forsyth, R. E. Hendrick, and R. L. Kelly, Phys. Rev. D **20**, 2839 (1979).
[6] D. M. Manley and E. M. Saleski, Phys. Rev. D **45**, 4002 (1992).
[7] G. Höhler, in *Pion-Nucleon Scattering*, edited by H. Schopper, Landolt-Börnstein New Series, Vol. I/9b, Parts 1 and 2 (Springer, Berlin, Heidelberg, New York, 1973).
[8] L. C. Liu, Acta Phys. Pol. B **24**, 1545 (1993).
[9] M. Clajus and B. M. K. Nefkens, πN Newsletter **7**, 76 (1992).
[10] D. Berley *et al.*, Phys. Rev. Lett. **15**, 641 (1965).
[11] D. M. Binnie *et al.*, Phys. Rev. D **8**, 2789 (1973).
[12] V. V. Abaev and S. P. Kruglov, Report No. PNPI 1794, St. Petersburg, 1992 (submitted to Z. Phys.).
[13] R. Ayed, Ph.D. thesis, CEA-N-1921, 1976.
[14] D. M. Manley, R. A. Arndt, Y. Goradia, and V. L. Teplitz, Phys. Rev. D **30**, 904 (1984).
[15] R. Bhandari and Y. Chao, Phys. Rev. D **15**, 192 (1977).
[16] AGS Proposal 909, W. J. Briscoe and W. B. Tippens, spokesmen, 1994.
[17] C. Wilkin, Phys. Rev. C **47**, R938 (1993); G. Faldt and C. Wilkin, Uppsala University, Report No. TSL/ISV-94-105, 1994 (unpublished).
[18] M. Arima, K. Shimizu, and K. Yazaki, Nucl. Phys. **A543**, 613 (1992).
[19] R. E. Chrien *et al.*, Phys. Rev. Lett. **60**, 2595 (1988).
[20] R. S. Kessler, Ph.D. thesis, UCLA, 1992.
[21] S. S. Kamalov, L. Tiator, and C. Bennhold, Phys. Rev. C **47**, 941 (1993).